



Characterization of Natural Fiber Extracted from *Sesbania rostrata*: An Alternative Potential for Synthetic Fibers

K. Raja¹, P. Senthilkumar², G. Nallakumarasamy³, T. Natarajan⁴

¹Department of Mechanical Engineering, K.S. Rangasamy College of Technology, Tiruchengode 637215, Tamil Nadu, India.

E-mail: rajamettur@gmail.com

²Department of Mechanical Engineering, K.S.R. College of Engineering, Tiruchengode 637215, Tamil Nadu, India.

E-mail: cryosenthil@yahoo.com

³Department of Mechanical Engineering, Excel Engineering College, Komarapalayam 637 303, Tamil Nadu, India.

E-mail: padnks@gmail.com

⁴Department of Mechanical Engineering, K.S. Rangasamy College of Technology, Tiruchengode 637215, Tamil Nadu, India

E-mail: natgobi@gmail.com

ABSTRACT

Enriching natural materials is essential for developing eco-friendly composites in structural and automotive applications. The aim of this work is to extensively characterize new natural cellulosic fiber extracted from *Sesbania rostrata* stem. *S. rostrata* fibers (SRFs) show cellulose content of 64.36 % with a range of tensile strength from 156 to 460 MPa and have a low density of 1.365 g/cm³. SRFs has crystallinity index of 58.41%, which is comparable with that of other common natural fibers. Furthermore, SRFs can resist the degradation of cellulose up to 246°C, which is revealed by thermogravimetric analysis.

Indexing terms/Keywords

Natural fiber; *Sesbania rostrata*; Thermogravimetric analysis; FTIR; XRD; Crystalline index

Academic Discipline And Sub-Disciplines

Mechanical Engineering, Chemistry, Composites

SUBJECT CLASSIFICATION

Natural fiber composites

TYPE (METHOD/APPROACH)

Characterization and Analysis

1. INTRODUCTION

Over the past two decades, synthetic fiber-reinforced polymer composites have been playing a vital role in the automobile, construction, aerospace, and food-packaging industries due to their excellent properties such as high mechanical strength, thermal stability, and chemical resistance^[1]. However, synthetic fibers have certain limitations such as non-biodegradable nature, high energy consumption, high cost, and associated health-related issues^[2]. In this context, materials researchers are striving to incorporate natural fibers instead of synthetic fibers in polymer composites due to their exotic properties such as biodegradability, adequate strength, eco-friendly aspect, abundance in nature, wide variety, cheapness, and low density^[2,3]. Natural fibers extracted from various parts of the plants, which include leaf, seed, fruit, root, straw, and stem, mainly comprise cellulose, hemicellulose, and noncellulosic components such as lignin, pectin, and wax^[4]. The quality of lignocellulosic fiber mainly depends on the crystalline nature of the cellulose, internal structure, chemical composition, density, and thermal stability^[5].

Sesbania rostrata (SR) is a leguminous crop from *Sesbania* genus of Fabaceae family, which consists of approximately 500 species. *S. rostrata* is native of West Africa and commonly known as *new dhaincha* in India^[6]. It is a fast growing green manure plant used as an intercrop, an alley crop, and a shading crop to maintain a healthy soil for better crop production. In addition, the stems of SR are used as firewood, as poles, and in light construction^[7]. To the best of our knowledge, none of the researchers have investigated the physicochemical, mechanical, and thermal properties of SR fiber.

2. MATERIALS AND METHODS

2.1 Extraction of SR fibers (SRFs)

SR plants are cultivated as an intercrop of turmeric field in the Erayamangalam region, Namakkal District, Tamil Nadu, India. The stems are separated from the SR and immersed in a water tank for 10 days at room temperature in order to

undergo microbial degradation^[8]. After water retting process, the fibers are manually extracted from the wet stem. The extracted fibers are washed several times with distilled water to remove the unwanted piths on their surface and dried under the sun to remove the moisture content present in the fiber. The extraction process of SR fibers (SRFs) is shown in Fig 1.

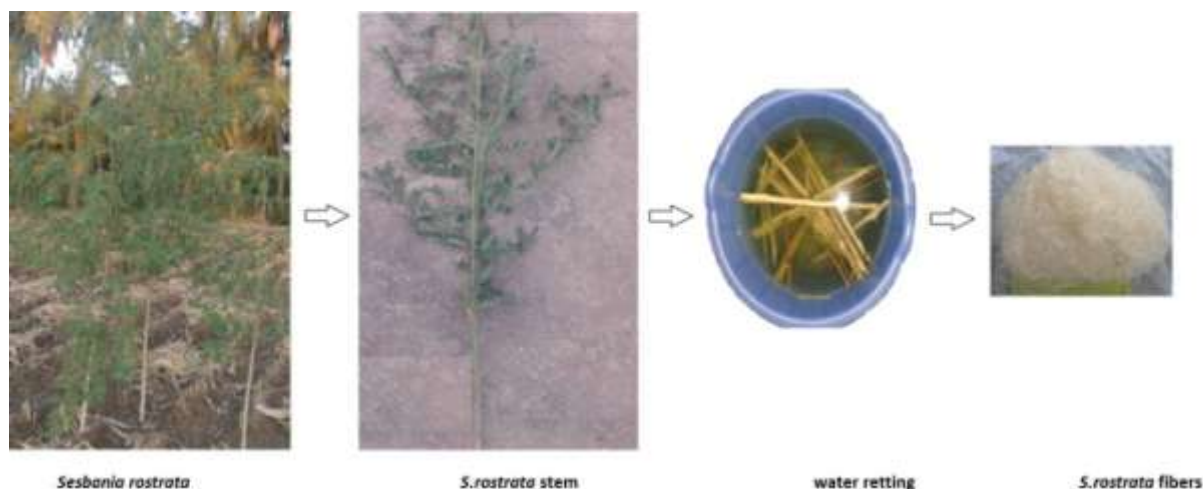


Fig 1: Extraction process of SRFs.

2.2 Characterization of the PFFs

2.2.1 Chemical compositional analysis in the SRFs

The chemical compositions such as cellulose, hemicellulose, and lignin content of the SRFs were determined at SITRA (South India Textile Research Association, Coimbatore, India) laboratory by the standard test procedures^[9]. Using Mettler Toledo XSZ05 balance method, we evaluated the density of SRFs^[10]. The wax content of the SRFs was assessed using Conrad procedure and their ash content was calculated as per the ASTM E1755-61 standard^[11,12]. Presence of moisture in the SRFs was determined by the conventional weight loss method^[13].

2.2.2 Tensile test of SRFs

The tensile properties of single SRFs were determined using an Instron 5500 Series Universal Tester (Instron Corp., Canton, MA) with the aid of 1 kN load cell in accordance with ASTM D3379-89 standards. To ensure the accuracy of the results, we tested a minimum of 25 single SRFs at a 50-mm gauge length with a crosshead speed of 0.5 mm/min. The entire test was carried out at an ambient temperature of 21 °C and the relative humidity was maintained at 61%^[14].

2.2.3 Fourier Transform-Infrared (FTIR) analysis

FTIR spectrum of the SRFs was captured by using an FTIR Spectrometer (Spectrum 100; PerkinElmer, Waltham, MA) to determine the free functional groups present in the fiber. The powdered fiber sample was mixed with potassium bromide at a ratio of 2:200 (w/w) and then pelletized by applying a hydraulic pressure of 125 kg cm⁻² for 1 min. The pelletized sample was analyzed with a scan rate of 32 scans per minute at a resolution of 2 cm⁻¹ in the wave number region of 500–4000 cm⁻¹^[12].

2.2.4 X-ray Diffraction spectroscopy

The crystallinity index (CrI) and crystallite size of SRFs were studied by X-ray diffraction (XRD) spectroscopy (X'Pert PRO; PANalytical, Almelo, the Netherlands) with monochromatic CuK α radiation of 0.154 nm wavelength at a current of 30 mA with an accelerating voltage of 40 kV. The analysis was carried out in the 2 θ ranges from 10° to 80° at a scanning speed of 5° per min^[15].

2.2.5 Thermogravimetric Analysis (TGA) of SRFs

The thermal stability of SRFs was determined from the thermograph obtained by heating the powder samples (10 mg) in a thermogravimetric analyzer (TGA Q50; TA Instruments, Tacoma, WA) at a rate of 20 °C/min from 30 to 800 °C. The experiment was carried out in the nitrogen atmosphere with a flow rate of 20 mL/min, and the samples were kept in an alumina crucible to avoid the temperature variations measured by the thermocouple.

2.2.6 Fiber surface morphology

The surface morphology of SRFs was examined using a scanning electron microscope (SEM; SUPRA Zeiss, Oberkochen, Germany). The fiber sample was coated with a thin gold layer to make its surfaces conductive and to avoid electron



charge gathering. The SEM studies were conducted by scanning the samples with a high-energy electron beam at an accelerating voltage of 10 kV in a vacuum chamber.

3. RESULTS AND DISCUSSION

3.1 Chemical composition of SRFs

The chemical composition and density of SRFs were summarized and compared with those of other common natural fibers in Table 1 [12,16,17].

Table 1. Chemical compositions of the raw SRFs compared with those of the other common natural fibers

Fiber	Cellulose (%)	Hemicellulose (%)	Lignin (%)	Wax (%)	Moisture (%)	Ash (%)	Density (g/cm ³)
SRFs	64.36	11.25	17.19	0.29	7.98	1.45	1.365
Artisdita hystrix leaf [16]	59.54	11.35	8.42	—	—	—	0.540
Prosopis juliflora [17]	61.65	16.14	17.11	0.61	9.48	5.2	0.580
Acacia leucophloea [17]	68.09	13.6	17.73	0.55	8.83	0.08	1.385
Areca fiber [12]	57.35–58.21	13–15.42	23.17–24.16	0.12	7.32	—	0.7–0.8
Bamboo [12]	26–43	30	21–31	—	8.9	—	0.6–1.1
Jute [12]	61–71	14–20	12–13	0.5	12	—	1.3
Banana [12]	60–65	19	5–10	—	—	—	1.35
Sisa [12]	65	12	9.9	2	11	—	1.5
Flax [12]	71	18.6–20.6	2.2	1.5	7	—	1.5

The variance existing between the chemical compositions of natural fibers is because of age and part of the plant where the fiber was extracted, extraction procedure, and soil and weather conditions [18]. The rich content of cellulose (64.36 wt%) tends to improve the mechanical properties of the SRF whereas the low hemicellulose content (11.25 wt%) tends to reduce the moisture absorption capacity and in turn increase the thermal stability of the fiber. The presence of lignin content (17.19 wt%) acts as a bonding agent between the cell wall structures to improve the rigidity and strength of the fiber. Less amount of wax content (0.29 wt%) in the fiber is desirable because it reduces the bonding characteristics between the fiber and polymer matrix in composites. The ash and moisture contents of the SRFs were found to be 1.45 and 7.98 wt%, respectively. The SRFs have low density (1.365 g/cm³) as compared to the E-glass (2.5 g/cm³) and carbon fibers (1.7 g/cm³), which is favorable for making lightweight composite components [12].

3.2 Tensile properties of SRFs

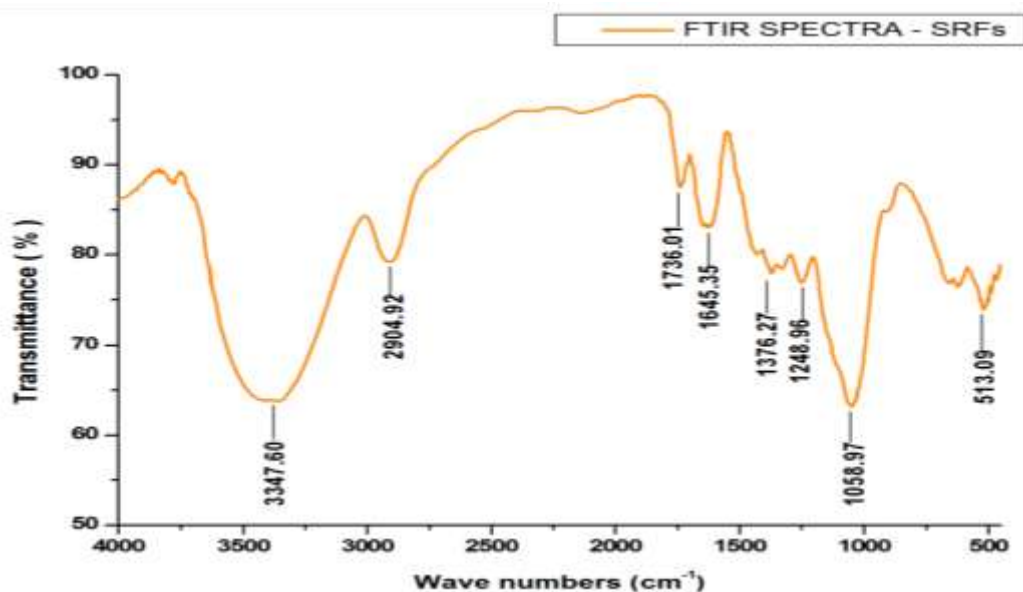
The mechanical properties of the natural fibers mostly depend on the percentage of cellulose content present in chemical composition and the cell wall structure, especially microfibril angle. The high cellulose content and small microfibril angle contribute in improving the tensile strength and stiffness of the fiber [19,20]. The mechanical properties of the SRFs were determined by performing the single-fiber tensile test using a universal tester. At the same time, the diameter of the SRFs was measured through an optical microscope with image software. The value of average fiber diameter was found to be 95±34 μm. The obtained tensile properties of SRFs were the following: tensile strength of 156–460 MPa, Young's modulus of 9.50–67.89 GPa, and strain at failure of 0.18%–3.78%. The tensile strength of areca, bamboo, sisal, banana, hemp, E-glass, and carbon fiber are 147–322, 140–230, 511–635, 355, 690, 2000–3500, and 2400–4000 MPa, respectively [12].

The microfibril angle (α) of the SRFs was calculated from Equation (1).

$$\varepsilon = \ln \left(1 + \frac{\Delta L}{L_0} \right) = -\ln(\cos \alpha) \quad (1)$$

Where α is the microfibril angle (deg.), ε the strain (no unit), L_0 the gauge length (mm), and ΔL the change in length (Final Length – L_0) (mm). The microfibril angle of the SRFs was found to be in the range of 3.52°–15.52° whereas microfibril angles of other natural fibers such as banana, flax, hemp and jute are 11°–12°, 5°, 6.2°, and 8.1°, respectively [20].

3.3 FTIR spectrum analysis of SRFs



The FTIR spectrum of the SRFs is shown in Fig 2.

Fig 2: FTIR spectrum of the SRFs

which illustrates a broad peak at 3347.60 cm^{-1} and sharp peaks at 2904.92 , 1736.01 , 1645.35 , 1376.27 , 1248.96 , 1058.97 , and 513.09 cm^{-1} . The broad peak observed at 3347.60 cm^{-1} corresponds to the stretching vibrational mode of intra- and intermolecular hydroxyl ($-\text{OH}$) bond of cellulose I and II^[9]. The stretching vibration of aliphatic saturated (CH), methylene (CH_2) and methyl (CH_3) groups in cellulose and hemicellulose components was observed at 2904.92 cm^{-1} ^[21]. The peak observed at 1736.01 cm^{-1} belongs to the stretching vibration of carbonyl ($\text{C}=\text{O}$) group from the ester (RCOOR') and carboxylic acid (RCOOH) in hemicellulose and lignin^[20]. The broad absorption band observed at 1645.35 cm^{-1} attributes to the dipole moment of alkenes ($\text{C}=\text{C}$) in lignin^[22]. The peak seen at 1376.27 cm^{-1} indicates the in-plane bending vibrations of the CH_2 and CH groups of cellulose.^[23] The CO group stretching in hemicellulose was observed at 1248.96 cm^{-1} .^[8] The broad peak observed at 1058.97 cm^{-1} is attributed to asymmetric vibrations of $\text{C}-\text{O}-\text{C}$ group in cellulose.^[23] The $\text{C}-\text{OH}$ bending is associated with the wave number of 513.09 cm^{-1} ^[22].

3.4 XRD spectrum analysis of SRFs

The X-ray powder diffraction pattern of the SRFs is shown in Fig 3.

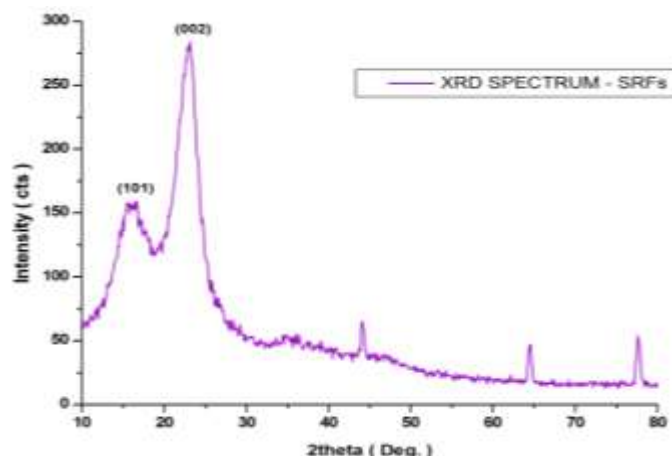


Fig 3: XRD spectrum of the SRFs.

The first highest intensity peak seen at $2\theta = 23.1^\circ$ corresponds to the (0 0 2) crystallographic plane. This peak confirms the presence of cellulose I in the SRFs. The second intensity peak observed at $2\theta = 16.7^\circ$ represents the (1 0 1) crystallographic plane. This peak shows the presence of hemicellulose and lignin in an amorphous form.^[24] The relative amount of ordered crystalline material in cellulose was calculated by using Segal's empirical Equation (2)^[25].



$$CrI(\%) = \left[\frac{I_{002} - I_{AM}}{I_{002}} \right] \times 100 \quad (2)$$

where CrI is crystallinity index in %, I_{002} the intensity count value at $2\theta = 23.1^\circ$, and I_{AM} the intensity count value at $2\theta = 18.9^\circ$. The obtained CrI of the SRFs is 58.41%, which is greater than that of *Ipomoea staphylinia* fibers (43.96 %) and smaller than that of jute (71%) and hemp (88%)^[8].

The average crystalline size (D) of the SRFs was computed by substituting the X-ray wavelength value as 0.154 nm in λ , K value as 0.94 (Scherrer constant), FWHM (full-width at half maximum) value at (0 0 2) crystallographic plane in β (radian), and θ value as Bragg's angle at peak intensity count in Scherrer Equation (3)^[26].

$$D = \frac{K\lambda}{\beta \cos \theta} \quad (3)$$

The computed crystalline size (D) of the SRFs is 4.32 nm, which is higher than that of Napier grass fiber (2.83 nm) and rice straw (3.75 nm) but smaller than that of hemp (4.5 nm) and flax (5.4 nm)^[27]. The CrI and crystalline size influence the chemical reactivity and water absorption capacity of the fiber^[9].

3.5 Thermogravimetric analysis of the SRFs

The thermal stability of the SRFs sample is studied by using thermogravimetry (TG) and differential thermogravimetry (DTG) curves, as shown in Fig 4.

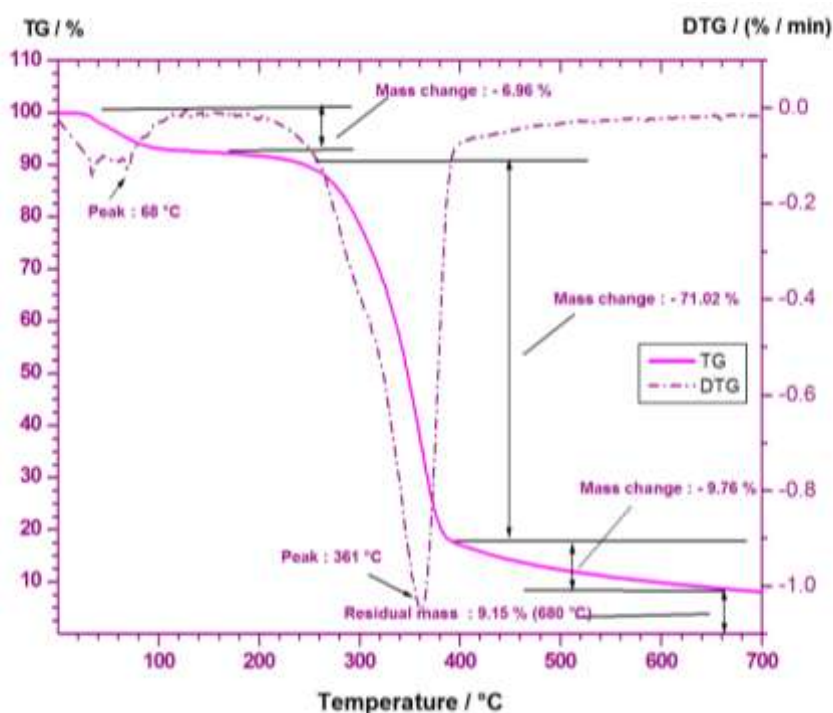


Fig 4: TG and DTG curves of the SRFs.

The TG curve clearly revealed three stages of mass losses of fiber sample with respect to increase in temperature. In the initial stage, moisture content in the fiber was evaporated when the temperature was raised from 32 to 89 °C with a mass loss of 6.96%^[8]. During the second stage, a minor mass loss of 3.11% up to 246 °C was recorded, which indicates that the fiber is thermally stable up to that temperature. The major mass loss of 71.02% was observed between the temperature range of 246 and 387 °C due to thermal decomposition and depolymerization of hemicellulose and cellulose at the peak temperature of 361 °C^[20]. It is comparable with the peak temperatures of 339.1, 308.2, 321, 309.2, and 298.2 °C corresponding to *Perotis indica*, hemp, bamboo, Kenaf, and jute, respectively^[15]. The final stage of degradation of fiber was attributed to the decomposition of lignin compound up to 680 °C with a mass loss of 9.76%. An ash content of 9.15% mass remains as residue in the sample. The activation energy (E_a) of the SRFs was computed by substituting the kinetic parameter in the Broido's Equation (4)^[20].

$$\ln \left[\ln \left[\frac{1}{y} \right] \right] = - \left(\frac{E}{R} \right) \left[\left(\frac{1}{T} \right) + K \right] \quad (4)$$

where R is (equal to 8.314 J/mol K) universal gas constant, K the constant, T the temperature in Kelvin, y the normalized weight (w/w_0), w_0 the initial weight of the fiber sample, and w_t the sample weight at any time t . The activation energy (97.96 kJ/mol) was determined from the slope of the line obtained by plot of $\ln[\ln(1/y)]$ vs $(1/T)$, as given in Fig 5.

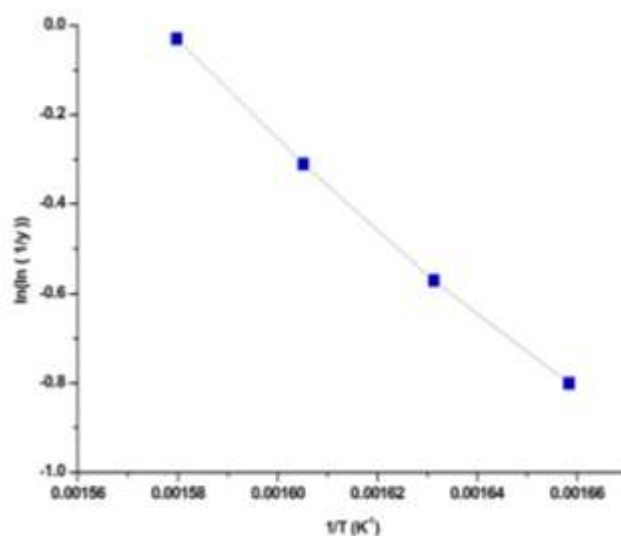


Fig 5: Broido's plot of the SRFs.

3.6 Surface morphology of the SRFs

The surface morphology of the raw SRFs was examined by the SEM image, as shown in Fig 6.

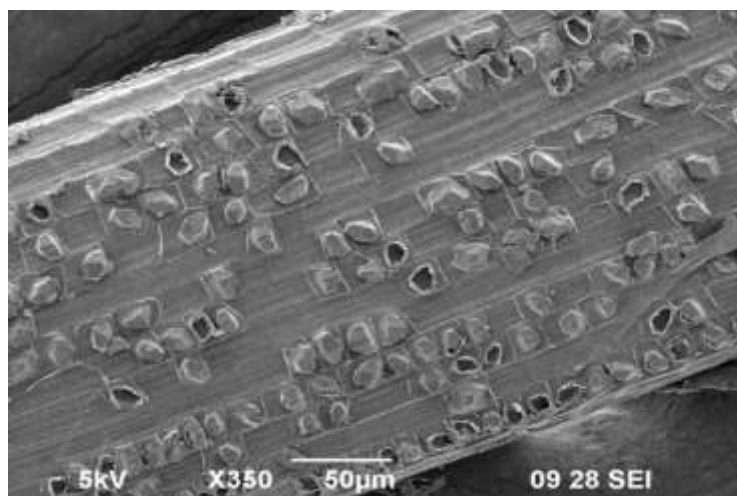


Fig 6: SEM image of the SRFs

Thin lines with tiny holes are observed on the entire surface of the fiber. The small ridge on the entire fiber surface shows the presence of lignin, hemicellulose, and trace amount of impurities that cover the cellulose^[28].

4. CONCLUSION

In this study, complete characterization of *S. rostrata* fiber was carried out. The obtained results showed that the fiber has high cellulosic content, which provides better mechanical strength. The chemical composition, density, and tensile strength of the SRFs were comparable with those of the other available natural fibers. Further, the tiny lined surface morphology and the high thermal stability of SRFs ensure better bonding with polymer resins for making composites under elevated temperature without degradation of the fiber. Hence, promising results of the SRFs showed that it could be a potential alternative to synthetic fibers for making light-weight and good-strength composites in a wide range of industrial applications.

ACKNOWLEDGMENTS

We gratefully acknowledge the support provided by DST-FIST (SR/FST/College – 235/2014, dated 21.11.14), Government of India, for carrying out this research work.



REFERENCES

1. Sathishkumar, T. P., S. Satheeshkumar, and J. Naveen. 2014. Glass fiber-reinforced polymer composites – a review. *J. Reinf. Plast. Compos.* 33(13): 1258–1275.
2. Wambua, P., J. Ivens, and I. Verpoest. 2003. Natural fibres: can they replace glass in fibre reinforced plastics? *Compos. Sci. Technol.* 63(9): 1259–1264.
3. Nirmal, U., J. Hashim, S. T. Lau, Y. My, and B. Yousif. 2012. Betelnut fibres as an alternative to glass fibres to reinforce thermoset composites: a comparative study. *Text. Res. J.* 82(11): 1107–1120.
4. Thakur, V. K., M. K. Thakur, and R. K. Gupta. 2014. Review: raw natural fiber-based polymer composites. *Int. J. Polym. Anal. Charact.* 19(3): 256–271.
5. Pickering, K. L., M. G. Aruan Efendy, and T. M. Le. 2015. A review of recent developments in natural fibre composites and their mechanical performance. *Compos. Part A Appl. Sci. Manuf.* 83: 98–112.
6. Shuguang, J. I. A. N., S. H. E. N. Weijun, and Y. A. N. G. Zhongyi. 2009. Enhanced adaptability of *Sesbania rostrata* to pb/zn tailings via stem nodulation. *J. Environ. Sci.* 21(8): 1135–1141.
7. Saraswati, R., T. Match, and J. Sekiya. 1992. Nitrogen-fixation of *Sesbania rostrata* – contribution of stem nodules to nitrogen acquisition. *Soil Sci. Plant Nutr.* 38(4): 775–780.
8. Santhanam, K., A. Kumaravel, S. S. Saravanakumar, and V. P. Arthanarieswaran. 2016. Characterization of new natural cellulosic fiber from the *Ipomoea staphylina* plant. *Int. J. Polym. Anal. Charact.* 21(3): 267–274.
9. Indran, S., R. Edwin Raj, and V. S. Sreenivasan. 2014. Characterization of new natural cellulosic fiber from *Cissus quadrangularis* root. *Carbohydr. Polym.* 110: 423–429.
10. Saravanan, N., P.S.Sampath, T.A.Sukantha and T.Natarajan. 2016. Extraction and Characterization of New Cellulose Fiber from the Agrowaste of Lagenaria Siceraria (Bottle Guard) Plant. *J. Adv. Chem.* 12(09):4382-4388.
11. Conrad, C. M. and M. Carl. 1944. Determination of wax in cotton fiber: a new alcohol extraction method. *Ind. Eng. Chem. Anal. Ed.* 16(12): 745–748.
12. Binoj, J. S., R. Edwin Raj, V. S. Sreenivasan, and G. Rexin Thusnavis. 2016. Morphological, physical, mechanical, chemical and thermal characterization of sustainable Indian areca fruit husk fibers (*Areca catechu* L.) as potential alternate for hazardous synthetic fibers. *J. Bionic Eng.* 13(1): 156–165.
13. Sathishkumar, T. P., P. Navaneethkrishnan, S. Shankar, and R. Rajasekar. 2013. Characterization of new cellulose *Sansevieria ehrenbergii* fibers for polymer composites. *Compos. Interf.* 20(80): 575–593.
14. Vignesh, V., A. N. Balaji, and M. K. V. Karthikeyan. 2016. Extraction and characterization of new cellulosic fibers from Indian mallow stem: an exploratory investigation. *Int. J. Polym. Anal. Charact.* DOI.10.1080/1023666X.2016.1175206.
15. Prithiviraj, M., R. Muralikannan, P. Senthamaraiannan, and S. S. Saravanakumar. 2016. Characterization of new natural cellulosic fiber from the *Perotis indica* plant. *Int. J. Polym. Anal. Charact.* DOI.10.1080/1023666X.2016.1202466.
16. Kathiresan, M., P. Pandiarajan, P. Senthamaraiannan, and S. S. Saravanakumar. 2016. Physicochemical properties of new cellulosic *Artisidita hystrix* leaf fiber. *Int. J. Polym. Anal. Charact.* DOI.10.1080/1023666X.2016.1194636.
17. Arthanarieswaran, V. P., A. Kumaravel, and S. S. Saravanakumar. 2015. Characterization of new natural cellulosic fiber from *Acacia leucophloea* bark. *Int. J. Polym. Anal. Charact.* 20(4): 367–376.
18. Keller, A., M. Leupin, V. Mediavilla, and E. Wintermantel. 2001. Influence of the growth stage of industrial hemp on chemical and physical properties of the fibers. *Ind. Crops Prod.* 13: 35–48.
19. Fidelis, A., M. Ernestina, and T. V. Castro Pereira. 2013. The effect of fiber morphology on the tensile strength of natural fibers. *J. Mater. Res. Technol.* 2(2): 149–157.
20. Natarajan, T., A. Kumaravel, and R. Palanivelu. 2016. Extraction and characterization of natural cellulosic fiber from *Passiflora foetida* stem. *Int. J. Polym. Anal. Charact.* DOI.10.1080/1023666X.2016.1168636.
21. Boopathi, L., P. S. Sampath, and K. Mysamy. 2012. Investigation of physical, chemical and mechanical properties of raw and alkali treated *Borassus fruit* fiber. *Compos. Part B Eng.* 43(8): 3044–3052.
22. Nagaraja Ganesh, B., and R. Muralikannan. 2016. Extraction and characterization of lignocellulosic fibers from *Luffa cylindrica* fruit. *Int. J. Polym. Anal. Charact.* 21(3): 259–266.
23. Nagaraja Ganesh, B., and R. Muralikannan. 2016. Physico-chemical, thermal, and flexural characterization of *Cocos nucifera* fibers. *Int. J. Polym. Anal. Charact.* 21(3): 244–250.



24. Mayandi, K., N. Rajini, P. Pitchipoo, JT Winowlin Jappes, and A. Varada Rajulu. 2016. Extraction and characterization of new natural lignocellulosic fiber *Cyperus pangorei*. *Int. J. Polym. Anal. Charact.* 21(2): 175–183.
25. Segal, L. G. J. M. A., J. J. Creely, A. E. Martin, and C. M. Conrad. 1959. An empirical method for estimating the degree of crystallinity of native cellulose using the X-ray diffractometer. *Text. Res. J.* 29(10): 786–794.
26. French, A. D., and M. S. Cintrón. 2013. Cellulose polymorphy, crystallite size, and the segal crystallinity index. *Cellulose* 20(1): 583–588.
27. Kommula, V. P., K. Obi Reddy, M. Shukla, T. Marwala, E. V. Subba Reddy, and A. Varada Rajulu. 2016. Extraction, modification, and characterization of natural ligno-cellulosic fiber strands from napier grass. *Int. J. Polym. Anal. Charact.* 20(1): 18–28.
28. Belouadah, Z., A. Ati, and M. Rokbi. 2015. Characterization of new natural cellulosic fiber from *Lygeum spartum* L. *Carbohydr. Polym.* 134: 429–437.

Author' biography with Photo



K.Raja received his postgraduate degree in CAD/CAM from Anna University, Chennai on 2008. He has academic experience of 14 years and Currently he is working as Assistant Professor, Department of Mechanical Engineering at K.S.Rangasamy College of Technology, Tiruchengode, India. His research interest is natural fiber reinforced composite materials. He has published articles in 6 national conferences.



Dr.P.Senthil Kumar, Professor & Head , Department of Mechanical Engineering at K.S.R. College of Engineering, Tiruchengode, India. He has academic experience of 21.5 years and Research experience of 16 years. He has received Ph.D. Degree from the IIT Madras, Chennai in the field of cryogenics.Under his guidance 14 scholars completed their Ph.D degree. He has published more than 53 international Journals, 15 national conferences, 48 International conferences and 60 national conferences.



Dr.G.Nallakumarasamy, Professor & Head , Department of Mechanical Engineering at Excel Engineering College, Komarapalayam, India. He has academic experience of 26 years and Research experience of 09 years. He has received Ph.D. Degree from the Anna University, Chennai in the field of process planning. He has published more than 04 international Journals, 06 International conferences and 04 national conferences.



T.Natarajan received his Master degree in CAD/CAM from Anna University, Chennai on 2006. He has academic experience of 10 years and currently he is working as Assistant Professor, Department of Mechanical Engineering, at K.S.Rangasamy College of Technology, Tiruchengode, India. His research interest is natural fiber reinforced biocomposites. He has published articles in 2 international journals and 3 national conferences.